# Morphometric Evaluation of Facial and Vestibulocochlear Nerves Using Magnetic Resonance Imaging in Patients with Menière's Disease

**Wilhelm Flatz** ( Wilhelm.Flatz@med.uni-muenchen.de )
University Hospital, LMU Munich
**Annika Henneberger**
HNO Zentrum Ulm
**Robert Gürkov**
HNO Am Rotkreuzplatz, Munich
**Regina Schinner**
University Hospital, LMU Munich
**Ullrich Mueller-Lisse**
University Hospital, LMU Munich
**Maximilian Reiser**
University Hospital, LMU Munich
**Birgit Ertl-Wagner**
Hospital for Sick Children

**Research Article**

**Keywords:** Morphometric evaluation, vestibulocochlear nerves, Magnetic Resonance Imaging, Menière's disease

**Posted Date:** August 9th, 2021

**DOI:** https://doi.org/10.21203/rs.3.rs-753415/v1

# Abstract

Several studies proposed a loss of neural structures (such as hair cells or neurons within the spiral ganglion) in Menière's disease (MD). It has been shown that VII$^{th}$ and VIII$^{th}$ cranial nerves are enlarged within MD patients compared to normal controls. We now aimed to investigate potential differences in these two nerves in patients with MD. Etiology of endolymphatic hydrops, central pathological hallmark of MD, includes genetic predisposition, autoimmune processes, viral infections, cellular apoptosis and oxidative stress. We evaluated morphometric properties (long and short diameter, cross-sectional area) of the VII$^{th}$ and VIII$^{th}$ cranial nerves passing from the cerebellopontine angle to the inner ear modiolus, acquired on a clinical 3T magnetic resonance imaging scanner.

71 patients with MD were included, 53 of whom clinically showed a unilateral affection. Our data showed no differences in nerve morphometry between the clinically non-affected and the clinically affected side in patients with clinically unilateral MD. There was also no correlation to duration of symptoms, in contrast to previously demonstrated correlations between clinical features and the extent of endolymphatic hydrops. A disease process starting before the onset of clinical symptoms could be a potential explanation.


# Introduction

Menière's disease (MD) is characterized by episodic vertigo associated with tinnitus, fluctuating hearing loss, aural fullness and endolymphatic hydrops (ELH) (1, 2). Several studies proposed a loss of neural structures (such as hair cells or neurons within the spiral ganglion) in Menière's disease (MD) (3–9). In recent years several studies have evaluated and quantified ELH in patients with MD (10–13). Only few studies, however, have analyzed morphometric parameters of cranial nerves VII and VIII on MRI (14–17).

The course of cranial nerves VII and VIII from the pons through the cerebellopontine angle and the internal auditory canal (IAC) make these nerves amenable to morphometric evaluation in anatomical and MRI studies. The VIII$^{th}$ cranial nerve divides within the IAC into its three branches: cochlear nerve (CN), superior vestibular nerve (SVN) and inferior vestibular nerve (IVN). In the anterosuperior portion of the IAC the facial nerve is found, and inferior to it the cochlear nerve (18–22). To our knowledge, no morphometric analyses of these nerves have been performed using different MRI sequences with different spatial resolution in patients with clinically unilateral MD in correlation to symptom duration.

We previously demonstrated a swelling of VII$^{th}$ and VIII$^{th}$ cranial nerves on MR imaging in patients with MD (17). The aim of this study was to investigate morphometric differences of the VII$^{th}$ and VIII$^{th}$ cranial nerve within MD patients using different MR imaging techniques.

# Methods

# Study group

Ethical review board approval was provided by the institutional review board of University of Munich / LMU Munich, Protocol-Nr. 093 – 09. All examinations were performed in concordance with the Helsinki Declaration revised 2013.

Patients with certain MD according to the AAO-HNS classification (1995)(23) and with MR morphologic confirmation of endolymphatic hydrops (ELH) as an equivalent to the required histopathological findings were included in the study (12, 24–26). All of these patients underwent MRI on a clinical 3 Tesla scanner investigation with a sequence protocol comprising several different MR sequences described below. All patients gave their informed consent for all the methods including them in the study, also for the locally enhanced inner ear MRI (LEIM) and the electrophysiological examinations. Morphometric analysis of the $VII^{th}$ and $VIII^{th}$ cranial nerves was performed retrospectively. 24 hours prior to the MRI scan a gadolinium-based contrast agent diluted 8-fold in saline solution, was intratympanically injected (27, 28). After administration, the patient remained in a supine position for another 30 minutes with the head turned approximately 45 degrees toward the contralateral side.

Patient data consisting of CISS-0.6-sequence measurements was compared in our previous study to clinical healthy controls (17). In the current study we compared the affected side with the non-affected side of unilaterally affected MD patients as well as the bilaterally affected MD patients vs. unilateral affected MD patients using the mentioned different MRI sequences.

# MR Imaging

All MR imaging examinations were performed on a 3T MR unit (Magnetom Verio, Siemens Healthcare, Erlangen, Germany) using a commercially available 4-channel flexible surface coil combined with an 8-channel head coil.

The following MR-sequences were acquired of the temporal bone:

CISS-0.6: A strongly T2-weighted constructive interference in steady state sequence (CISS) with the following parameters was used: TR 7.2 ms, TE 3.16 ms, flip angle of 70°, field of view of 192 x 192 mm², matrix size of 320 x 320, averages 1 and slice thickness of 0.6 mm.

CISS-0.4: The second CISS had the following parameters: TR 6.24 ms, TE 2.87 ms, flip angle of 70°, field of view of 160 x 160 mm², matrix size of 320 x 320, averages 1 and slice thickness of 0.4 mm.

IR-0.5: The inversion recovery sequence was acquired using the following parameters: TR 6000 ms, TE 155 ms, flip angle of 180°, field of view of 160 x 160 mm², matrix size of 320 x 320, averages 1 and slice thickness of 0.5 mm.

IR-0.3: The second inversion recovery sequence had the following parameters: TR 6000 ms, TE 155 ms, flip angle of 180°, field of view of 160 x 160 mm², matrix size of 256 x 256, averages 1 and slice thickness of 0.3 mm.

# Analysis

We used a commercially available DICOM-Viewer (OsiriX v.4.0, 64-bit version, Pixmeo, Switzerland) for measuring the diameters of the VII$^{th}$ and VIII$^{th}$ cranial nerves. Consistent windowing levels and thin slice thickness were used performing transverse reformats at different locations throughout the course of the nerves from the cerebellopontine angle (CPA) to the internal auditory canal (IAC) fundus. Locations of the transverse sections were defined as follows:

- VIII – CPA,

- CN, SVN and IVN - meatus of the IAC;

- VII – CPA, meatus of the IAC, fundus of the IAC.

On each transverse section the long diameter (LD), short diameter (SD) perpendicular to LD and cross-sectional area (CSA) were measured. Several dot-markers were positioned on the outline of the examined nerves. These markers were linked and the CSA was calculated. All measurements were performed by the same two readers based on consensus readings. Both readers were blinded for the diagnosis of the patients. All these measurements were made for the CISS-0.4, the CISS-0.6, the IR-0.3 and the IR-0.5 sequences to investigate different nerve sizes depending on the used MRI sequence.

All patients received locally enhanced inner ear MRI (LEIM). The study group was subdivided into two cohorts: The first cohort consisted of unilaterally affected MD patients; the second consisted of bilaterally affected MD patients.

For comparing the affected and the clinically non-affected side a paired samples (dependent) t-test was employed using MedCalc v.12.7.2 (MedCalc Software bvba, Belgium) and SAS v. 9.4 for Windows (Copyright SAS Institute Inc., Cary, NC, USA). After Bonferroni correction $P < 0.05$ was reduced to $P < 0.000595$ for statistical significance. For comparing the subgroups of different symptom duration a two-sided independent samples t-test was used. Furthermore we used Scatterplots, Pearson Correlation Coefficients and Bland-Altman plots for visualization of the degree of correlation as well as measurement differences between the employed MRI sequences.

# Results

Both ears of the 71 MD patients (27 females, 44 males, mean age 54.4 years, age range 23–77 years) were measured and analysed. 53 of these patients were classified as unilaterally affected (20 females, 33 males, mean age 50.5 years, age range 23–77 years).

Clinical patient`s data including age and sex, the investigated LEIM-side, symptom duration, four-tone average calculated from the hearing at 0.5, 1, 2 and 3 kHz, cervical vestibular evoked myogenic potentials (cVEMP´s), electrocochleography data and caloric canal paresis including the measurements of the slow

phase speed (SPS, °/s) is shown in Table 1 for the unilaterally affected and in Table 2 for bilaterally affected MD patients.

No significant differences were observed when comparing the affected side to the non-affected side of the VII$^{th}$ and VIII$^{th}$ cranial nerves in the cohort of clinically unilaterally affected MD patients (Table 3) when adjusting for multiple testing. Without adjustment for multiple testing, in order for catering for an explorative approach, significant differences were found following no certain pattern, e.g. $p < 0.05$ could be found for SD at the level of CPA in the VIII$^{th}$ nerve and LD at level of CPA and fundus of the VII$^{th}$ nerve. These results were found to be independent of the used MRI sequence (CISS-0.4, CISS-0.6, IR-0.5 or IR-0.3) when adjusting for multiple testing (Tables 4 and 5) at the level of the CPA. Without Bonferroni correction significant differences were found in the VIII$^{th}$ nerve at this level only for SD in CISS-0.4 and CSA in IR-0.3 at the level of CPA (Table 3), obviously also not following a specific pattern.

Also, no significant differences between the morphometric measurements of the VII$^{th}$ and VIII$^{th}$ cranial nerves of the different sides were observed after Bonferroni correction in the cohort of clinically bilaterally affected patients.

When comparing the affected side of the unilaterally affected cohort with the LEIM-assessed side of the bilaterally affected cohort, no significant difference was shown along our measuring points of VII$^{th}$ and VIII$^{th}$ cranial nerves (Table 6, cross sectional areas within CISS-0.4, CISS-0.6, IR-0.3 and IR-0.5). Similar results were found investigating the clinically non-affected side of the first cohort and the contralateral ear of the bilaterally affected cohort. These results were again independent of the used MRI sequence.

An overview of the significant p-values without adjustment for multiple testing is summarized in Table 7, no specific pattern is recognizable.

We furthermore evaluated the morphometric properties of the VII$^{th}$ and VIII$^{th}$ cranial nerves of the first cohort in dependence of symptom duration. We initially divided the cohort of unilaterally affected patients in a subgroup with a symptom duration of a maximum of 12 months (n = 9) and compared these to the rest of the group (n = 26); we observed no significant differences between the groups neither when comparing the affected sides nor when comparing the non-affected sides. Subsequently, we compared patients with a symptom duration of at least 120 months (n = 14) to the patients with a symptom duration of a maximum of 12 months (n = 9). Again, there were no significant differences for the morphometric parameters (Table 8).

Scatterplots (diagrams 1–4), Pearson Correlation Coefficients (tables 9 and 10) and Bland-Altman plots (diagrams 5–8) were used for visualization of the degree of correlation as well as differences of measurements between each two of the 4 employed sequences.

# Discussion

In our patient cohorts we observed no significant differences between the clinically non-affected side and the clinically affected side of unilaterally affected patients with MD independently of the used MRI sequence when using the Bonferroni correction for multiple testing.

The pathogenesis of MD is still incompletely understood and the disease can be difficult to diagnose in early stages (29). Autoimmune processes and viral infections, such as latent herpes simplex virus type-1 that may cause vestibular neuritis (30), may play a role in the induction of MD. The involved immunological mechanisms are still not clear, but approximately one-third of the MD cases may have an autoimmune origin (31–35). Further pathophysiological aspects have been discussed, such as genetic predisposition (36–38), excitotoxicity, chronic otitis media (33), cellular apoptosis and oxidative stress. Reactive oxygen species, specifically nitric oxide generated by nitric oxide synthase, regulate the cochlear blood flow and lead to the release of mitochondrial cytochrome c, which is an important mediator of the intrinsic pathway of apoptosis (39, 40). The presence of hydrops may thus cause neuronal damage in the inner ear via a process of excitotoxicity (2). This neuronal damage could possibly affect the VIII$^{th}$ and potentially also the VII$^{th}$ cranial nerve.

Our data, however, demonstrated no differences in nerve diameters when comparing the clinically non-affected to the clinically affected side of unilaterally affected MD patients, possibly pointing toward a more systemic process that leads to subclinical reaction of the contralateral ear in clinically unilaterally affected MD patients. Kariya et al found equal results when comparing the mean number of spiral ganglion cells, the mean loss of inner and outer hair cells in patients and the damage of the stria vascularis with unilateral MD (6). This may support autoimmune processes or genetic predispositions, whereas local processes such as excitotoxicity and reactive oxygen species seem less likely. Moreover, our data did not show a correlation to clinical symptom duration, which again may point toward a very longstanding underlying process prior to the onset of clinical symptoms. On the other hand, it could also indicate that there is no change in the 7th and 8th cranial nerves in MD. However, this contradicts our previous study, which showed thicker nerves in patients with MD compared to a healthy control group (17).

Moreover our data showed different means for the same patients at the same measuring levels in dependence of the employed MRI sequence. These differences occur due to different variable sequence parameters such as slice thickness, different partial volume effects and the relatively small sample size. Where measurements varied largely between VII$^{th}$ and VIII$^{th}$ cranial nerve, differences between the 4 employed sequences were small. However, due to the limited sample size, a significant positive correlation (Tables 7 and 8) could only be shown for the IR-0.3 and IR-0.5 for VII$^{th}$ and VIII$^{th}$ cranial nerve. This reflects the difficulty of comparing absolute morphometric parameters in different MRI-studies performed with different sequences on different scanners.

In an explorative approach, without catering for multiple testing, scattered single parameters were found to be significant, these findings showed no specific pattern. Therefore Bonferroni correction was applied.

# Study Limitations

Our study has several limitations that need to be taken into account when interpreting the data. First, our sample size was limited, especially when performing the subgroup analyses. Larger studies are warranted to confirm our results. Second, we did not compare our measurements to an age- and sex-matched healthy control cohort to analyze differences to a clinically unaffected control population. As shown in our previous study (17) only few surveys (14–16, 22) with measurements of the VII$^{th}$ and VIII$^{th}$ cranial nerves had been published, mostly in normal hearing patients. The comparison of these published data also showed differences of nerve diameters according to the measuring point and the used MRI sequence.

# Conclusion

Our data showed no significant differences in diameters and cross-sectional areas of the VII$^{th}$ and VIII$^{th}$ cranial nerves between the affected and the clinically non-affected side of unilaterally affected patients with MD after Bonferroni correction for multiple testing. There was also no correlation to duration of clinical symptoms. This may potentially point toward a systemic process starting long before the onset of first clinical symptoms. On the other hand, it could also indicate that there is no change in the 7th and 8th cranial nerves in MD. However, this contradicts our previous study, which showed thicker nerves in patients with MD compared to a healthy control group (17).

Normative nerve diameters should only be used if comparable MRI sequence parameters are used as our data showed different means for the same patients at the same measuring points depending on the MRI sequences used.

# References


1. Syed, I. & Aldren, C. Meniere's disease: an evidence based approach to assessment and management. *International journal of clinical practice*, **66** (2), 166–170 (2012).
2. Semaan, M. T., Alagramam, K. N. & Megerian, C. A. The basic science of Meniere's disease and endolymphatic hydrops. *Current opinion in otolaryngology & head and neck surgery*, **13** (5), 301–307 (2005).
3. Spoendlin, H. *et al.* Multicentre evaluation of the temporal bones obtained from a patient with suspected Meniere's disease. *Acta oto-laryngologica Supplementum*, **499**, 1–21 (1992).
4. Merchant, S. N., Rauch, S. D. & Nadol, J. B. Jr Meniere's disease. European archives of oto-rhino-laryngology: official journal of the European Federation of Oto-Rhino-Laryngological Societies (EUFOS) : affiliated with the German Society for Oto-Rhino-Laryngology -. *Head and Neck Surgery*, **252** (2), 63–75 (1995).
5. Tsuji, K. *et al.* Temporal bone studies of the human peripheral vestibular system. Meniere's disease. *The Annals of otology, rhinology & laryngology Supplement*, **181**, 26–31 (2000).

6. Kariya, S. *et al.* Histopathologic changes of contralateral human temporal bone in unilateral Meniere's disease. Otology & neurotology: official publication of the American Otological Society, American Neurotology Society [and] European Academy of Otology and Neurotology. 2007;28(8):1063-8.
7. Megerian, C. A. Diameter of the cochlear nerve in endolymphatic hydrops: implications for the etiology of hearing loss in Meniere's disease., **115** (9), 1525–1535 (2005).
8. Schuknecht, H. F. The pathophysiology of Meniere's disease. *The American journal of otology*, **5** (6), 526–527 (1984).
9. Vasama, J. P. & Linthicum, F. H. Jr Meniere's disease and endolymphatic hydrops without Meniere's symptoms: temporal bone histopathology. *Acta oto-laryngologica*, **119** (3), 297–301 (1999).
10. Gurkov, R. *et al.* MR volumetric assessment of endolymphatic hydrops. *European radiology*, **25** (2), 585–595 (2015).
11. Pyykko, I., Nakashima, T., Yoshida, T., Zou, J. & Naganawa, S. Meniere's disease: a reappraisal supported by a variable latency of symptoms and the MRI visualisation of endolymphatic hydrops.BMJ open. 2013;3(2).
12. Gurkov, R., Flatz, W., Ertl-Wagner, B. & Krause, E. Endolymphatic hydrops in the horizontal semicircular canal: a morphologic correlate for canal paresis in Meniere's disease., **123** (2), 503–506 (2013).
13. Gurkov, R. *et al.* Herniation of the membranous labyrinth into the horizontal semicircular canal is correlated with impaired caloric response in Meniere's disease. Otology & neurotology: official publication of the American Otological Society, American Neurotology Society [and] European Academy of Otology and Neurotology. 2012;33(8):1375-9.
14. Jaryszak, E. M., Patel, N. A., Camp, M., Mancuso, A. A. & Antonelli, P. J. Cochlear nerve diameter in normal hearing ears using high-resolution magnetic resonance imaging., **119** (10), 2042–2045 (2009).
15. Nakamichi, R. *et al.* Establishing Normal Diameter Range of the Cochlear and Facial Nerves with 3D-CISS at 3T. Magnetic resonance in medical sciences: MRMS : an official journal of Japan Society of Magnetic Resonance in Medicine. 2013.
16. Kang, W. S. *et al.* Normative diameters and effects of aging on the cochlear and facial nerves in normal-hearing Korean ears using 3.0-tesla magnetic resonance imaging., **122** (5), 1109–1114 (2012).
17. Henneberger, A., Ertl-Wagner, B., Reiser, M., Gurkov, R. & Flatz, W. Morphometric evaluation of facial and vestibulocochlear nerves using magnetic resonance imaging: comparison of Meniere's disease ears with normal hearing ears. European archives of oto-rhino-laryngology: official journal of the European Federation of Oto-Rhino-Laryngological Societies (EUFOS) : affiliated with the German Society for Oto-Rhino-Laryngology -. *Head and Neck Surgery*, **274** (8), 3029–3039 (2017).
18. Glastonbury, C. M. *et al.* Imaging findings of cochlear nerve deficiency. *AJNR American journal of neuroradiology*, **23** (4), 635–643 (2002).

19. Sheth, S. & Branstetter BFt, Escott, E. J. Appearance of normal cranial nerves on steady-state free precession MR images. *Radiographics: a review publication of the Radiological Society of North America, Inc*, **29** (4), 1045–1055 (2009).
20. Rubinstein, D., Sandberg, E. J. & Cajade-Law, A. G. Anatomy of the facial and vestibulocochlear nerves in the internal auditory canal. *AJNR American journal of neuroradiology*, **17** (6), 1099–1105 (1996).
21. Guclu, B. *et al.* Anatomical study of the central myelin portion and transitional zone of the vestibulocochlear nerve. *Acta neurochirurgica*, **154** (12), 2277–2283 discussion 83. (2012).
22. Giesemann, A. M. *et al.* Improved imaging of cochlear nerve hypoplasia using a 3-Tesla variable flip-angle turbo spin-echo sequence and a 7-cm surface coil., **124** (3), 751–754 (2014).
23. Committee on Hearing and Equilibrium guidelines for the diagnosis and evaluation of therapy in Meniere's disease. American Academy of Otolaryngology-Head and Neck Foundation, Inc. Otolaryngology–head and neck surgery: official journal of American Academy of Otolaryngology-Head and Neck Surgery. 1995;113(3):181-5.
24. Gurkov, R. *et al.* Endolymphatic hydrops in patients with vestibular migraine and auditory symptoms. European archives of oto-rhino-laryngology: official journal of the European Federation of Oto-Rhino-Laryngological Societies (EUFOS) : affiliated with the German Society for Oto-Rhino-Laryngology -. *Head and Neck Surgery*, **271** (10), 2661–2667 (2014).
25. Gurkov, R., Pyyko, I., Zou, J. & Kentala, E. What is Meniere's disease? A contemporary re-evaluation of endolymphatic hydrops. *Journal of neurology*, **263** (Suppl 1), S71–81 (2016).
26. Nakashima, T. *et al.* Meniere's disease. *Nature reviews Disease primers*, **2**, 16028 (2016).
27. Jerin, C., Krause, E., Ertl-Wagner, B. & Gurkov, R. Longitudinal assessment of endolymphatic hydrops with contrast-enhanced magnetic resonance imaging of the labyrinth. Otology & neurotology: official publication of the American Otological Society, American Neurotology Society [and] European Academy of Otology and Neurotology. 2014;35(5):880-3.
28. Gurkov, R. *et al.* In vivo visualized endolymphatic hydrops and inner ear functions in patients with electrocochleographically confirmed Meniere's disease. Otology & neurotology: official publication of the American Otological Society, American Neurotology Society [and] European Academy of Otology and Neurotology. 2012;33(6):1040-5.
29. Paparella, M. M. & Djalilian, H. R. Etiology, pathophysiology of symptoms, and pathogenesis of Meniere's disease. *Otolaryngologic clinics of North America*, **35** (3), 529–545 vi. (2002).
30. Arbusow, V. *et al.* Latency of herpes simplex virus type-1 in human geniculate and vestibular ganglia is associated with infiltration of CD8 + T cells. *Journal of medical virology*, **82** (11), 1917–1920 (2010).
31. Greco, A. *et al.* Meniere's disease might be an autoimmune condition? *Autoimmunity reviews*, **11** (10), 731–738 (2012).
32. Filipo, R., Mancini, P. & Nostro, G. Ménière's disease and autoimmunity. *Annals of the New York Academy of Sciences*, **830**, 299–305 (1997).

33. Paparella, M. M., de Sousa, L. C. & Mancini, F. Meniere's syndrome and otitis media., **93** (11 Pt 1), 1408–1415 (1983).
34. Derebery, M. J. & Berliner, K. I. Prevalence of allergy in Meniere's disease. *Otolaryngology–head and neck surgery: official journal of American Academy of Otolaryngology-Head and Neck Surgery*, **123** (1 Pt 1), 69–75 (2000).
35. Derebery, M. J., Rao, V. S., Siglock, T. J., Linthicum, F. H. & Nelson, R. A. Menière's disease: an immune complex-mediated illness?, **101** (3), 225–229 (1991).
36. Klockars, T. & Kentala, E. Inheritance of Meniere's disease in the Finnish population. *Archives of otolaryngology–head & neck surgery*, **133** (1), 73–77 (2007).
37. Arweiler, D. J., Jahnke, K. & Grosse-Wilde, H. [Meniere disease as an autosome dominant hereditary disease]. *Laryngo- rhino- otologie*, **74** (8), 512–515 (1995).
38. de Kok, Y. J. *et al.* A Pro51Ser mutation in the COCH gene is associated with late onset autosomal dominant progressive sensorineural hearing loss with vestibular defects. *Human molecular genetics*, **8** (2), 361–366 (1999).
39. Hess, A. *et al.* Expression of inducible nitric oxide synthase (iNOS/NOS II) in the cochlea of guinea pigs after intratympanical endotoxin-treatment. *Brain research*, **830** (1), 113–122 (1999).
40. Kong, W. J., Ren, T. & Nuttall, A. L. Electrophysiological and morphological evaluation of the acute ototoxicity of sodium nitroprusside. *Hearing research*, **99** (1–2), 22–30 (1996).

# Tables

Due to technical limitations, tables are only available as a download in the Supplemental Files section.

# Figures

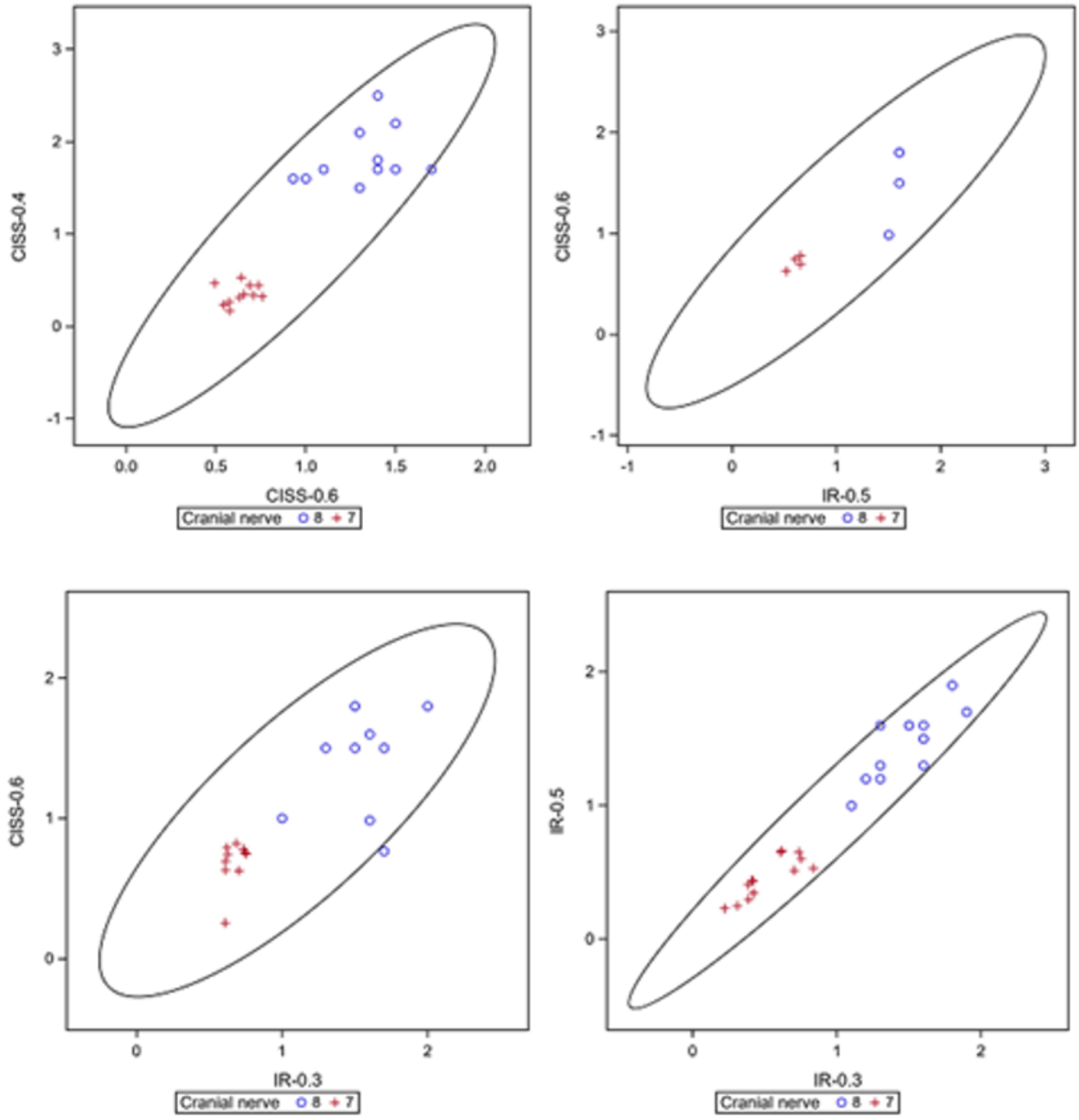


## Figure 1

Diagrams 1-4: Scatterplots with 95%-prediction ellipse visualizing the degree of correlation between each two of the 4 employed sequences (CISS-0.4, CISS-0.6, IR-0.3 and IR-0.5). 1. Degree of correlation between sequence CISS-0.4 and CISS-0.6 (upper left diagram). 2. Degree of correlation between sequence CISS-0.6 and IR-0.5 (upper right diagram). 3. Degree of correlation between sequence CISS-0.6 and IR-0.3 (lower left diagram. 4. Degree of correlation between sequence IR-=0.5 and IR-0.3 (lower right diagram).

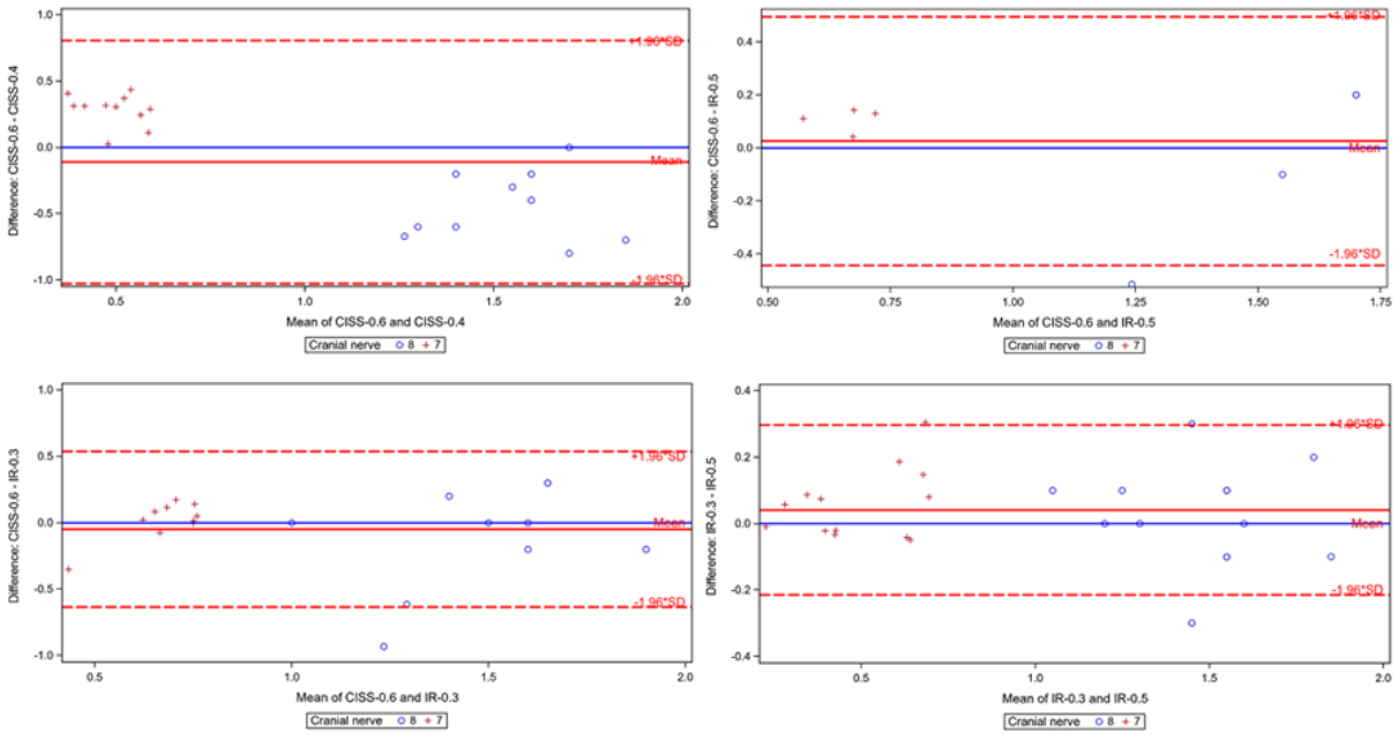


**Figure 2**

Diagrams 5-8: Bland-Altman-plots for each two of the 4 employed sequences visualizing the degree of correlation as well as differences of measurements between each two of the 4 employed sequences (CISS-0.4, CISS-0.6, IR-0.3 and IR-0.5). 5. Degree of correlation (x-axis) and differences of measurements (y-axis) between sequence CISS-0.6 and CISS-0.4 for cranial nerves VII and VIII (upper left diagram). 6. Degree of correlation (x-axis) and differences of measurements (y-axis) between sequence CISS-0.6 and IR-0.5 for cranial nerves VII and VIII (upper right diagram). 7. Degree of correlation (x-axis) and differences of measurements (y-axis) between sequence CISS-0.6 and IR-0.3 for cranial nerves VII and VIII (lower left diagram). 8. Degree of correlation (x-axis) and differences of measurements (y-axis) between sequence IR-0.3 and IR-0.5 for cranial nerves VII and VIII (lower right diagram).

# Supplementary Files

This is a list of supplementary files associated with this preprint. Click to download.

- Table1.jpg
- Table2.jpg
- Table3.jpg
- Table4.jpg
- Table5.jpg
- Table6.jpg

- Table7.jpg
- Table8.jpg
- Table9.jpg
- Table10.jpg